Louisiana State University
LSU Digital Commons

Faculty Publications Department of Physics & Astronomy

5-13-1996

Role of the environment in chaotic quantum dynamics

B. S. Helmkamp
Louisiana State University

D. A. Browne
Louisiana State University

Follow this and additional works at: https://digitalcommons.lsu.edu/physics_astronomy_pubs

Recommended Citation

Helmkamp, B., & Browne, D. (1996). Role of the environment in chaotic quantum dynamics. *Physical Review Letters, 76* (20), 3691-3694. https://doi.org/10.1103/PhysRevLett.76.3691

This Article is brought to you for free and open access by the Department of Physics & Astronomy at LSU Digital Commons. It has been accepted for inclusion in Faculty Publications by an authorized administrator of LSU Digital Commons. For more information, please contact ir@lsu.edu.

arXiv:chao-dyn/9510006v1 12 Oct 1995

Submitted to Physical Review Letters

The Role of the Environment in Chaotic Quantum Dynamics

B. S. Helmkamp and D. A. Browne

Department of Physics and Astronomy

Louisiana State University

Baton Rouge LA 70803–4001

()

Abstract

We study how the interaction with an external incoherent environment induces a crossover from quantum to classical behavior for a particle whose classical motion is chaotic. Posing the problem in the semiclassical regime, we find that noise produced by the bath coupling rather than dissipation is primarily responsible for the dephasing that results in the "classicalization" of the particle. We find that the bath directly alters the phase space structures that signal the onset of classical chaos. This dephasing is shown to have a semiclassical interpretation: the noise renders the interfering paths indistinguishable and therefore incoherent. The noise is also shown to contribute to the quantum inhibition of mixing by creating new paths that interfere coherently.

PACS Nos.: 05.45.+b, 03.65.Sq

Typeset using REVTEX

When a classically chaotic Hamiltonian system is treated quantum mechanically, many of the features associated with the classical chaos are suppressed [1]. Since we generally expect that classical behavior appears as the ray optics limit of quantum mechanics, it is interesting to ask how the mixing behavior [2] of classical chaos emerges in this limit. This question has been the subject of much recent study, leading to arguments that coarse-graining is sufficient for classical features to appear [3] while others insist that the coupling to an external environment is required [4]. It has also been suggested [5] that under certain conditions the quantum suppression of chaos will lead to a breakdown of the correspondence principle.

In the semiclassical limit, the quantum inhibition of mixing arises primarily from interference between classical paths [6]. Thus the proliferation of paths associated with the onset of mixing can lead to nonclassical behavior, and ultimately the collapse of the semiclassical picture, much sooner than were the motion not chaotic [7]. Actually, this depends more on the nature of the folding of the Lagrangian manifold in phase space [8] than on a sheer abundance of paths [9]. For example [10], long-lived nonclassical behavior can occur long before the chaos is fully developed in a one-dimensional time-dependent system when "false caustics," or folds not associated with classical turning points, appear.

In previous work [10,11] on an isolated quantum degree of freedom, we showed that one could identify specific quantum corrections to the classical chaotic dynamics associated with specific features of the classical phase space. The quantum and classical descriptions were essentially identical for motion in the vicinity of elliptic fixed points, where the evolving Lagrangian manifold wraps up into a "whorl." [7] In contrast, the quantum dynamics near the "tendrils" [7] associated with hyperbolic fixed points differs strongly from the classical description due to interference between the folds in the Lagrangian manifold that characterize this structure. Since these folds represent different classical paths that reach the same final point X, and the phase of each path's contribution to the semiclassical wavefunction [12,13] is given by the classical action, a nodal structure [10] appears when the difference in action between any two folds is a smooth function of X with magnitude of order $\hbar$.

Given the mechanisms that inhibit mixing in an isolated system, one might then ask what environment-related factors could undermine them, since we would expect [14] coupling to the environment to make a quantum object behave more classically. For example, Caldeira and Leggett [15] showed that the environment reduces the tunneling rate from a metastable well by lengthening the effective distance between turning points for resonant motion. Presumably, such "classicalization" [16] by the environment is what keeps the underlying quantum nature of macroscopic chaos from prevailing at long times [4,7]. In this context, the questions to address are how strong must the coupling to the environment be to accomplish this dephasing, and what determines the characteristic dephasing time.

One way to model the environment's influence is to add a randomly fluctuating, classical noise force to the Hamiltonian. In this manner Ott *et al.* [17] found the chaotic dynamics of the quantum kicked rotor to be strongly affected by weak amplitude-modulated noise, especially in the semiclassical regime, while Adachi *et al.* [16] demonstrated that frequency-modulated noise induces mixing behavior, even before complete classicalization occurs, for a wide range in the noise intensity. Scharf and Sundaram [18] have shown that classical noise also destroys the "scars" [19] (regions of enhanced amplitude that reflect the nonmixing nature of quantum mechanics) in the quasi-stationary [20] states of the quantum kicked rotor. However, this approach does not account for the fact that the quantum degree of freedom and the environment together form a closed system. More properly, the environment should be treated as a large collection of degrees of freedom that act in a deterministic fashion while reacting to the motion of the primary degree of freedom, resulting in dissipation as well as noise [21].

In this Letter we study the influence of the environment on a quantum particle moving in a cosine potential while being driven chaotic by an external time-dependent force. To model the environment more realistically, we treat it [15,22] as a bath of oscillators linearly coupled to the primary degree of freedom so that when parameterized appropriately it produces viscous damping and white noise in the classical limit. The hypothesis is that mixing, though disallowed in Hilbert space on first principles, is permitted in the reduced

Hilbert space of the particle when the bath has been integrated out.

The Hamiltonian of the isolated particle is

$$H_o(P, X, t) = P^2 - \frac{1}{2}\cos(\pi X) - \epsilon \sin(\omega_o t)X. \tag{1}$$

We pose the problem in the naive semiclassical limit with $\hbar = 1/200\pi$ where one can construct a well-localized wave packet and an effectively equivalent classical probability distribution to describe the particle's initial state. Our initial state is a narrow Gaussian wave packet at $(P_o, X_o) = (-0.397, 0.067)$ (see Fig. 1), and we choose $\epsilon = 0.126$ and $\omega_o = 2.5$ for which the long-time behavior [23] is chaotic.

Including the environmental degrees of freedom gives a total Hamiltonian [15]

$$H = H_o + \sum_\alpha \frac{f_\alpha}{2}\left\{\frac{p_\alpha^2}{\omega_\alpha^2} + \Big(x_\alpha - X\Big)^2\right\}. \tag{2}$$

In the classical limit, the particle obeys an equation of motion with damping constant η and noise $f(t)$

$$\frac{1}{2}\ddot{X} = -\frac{\partial H_o}{\partial X} - \eta\dot{X} + f(t) \tag{3}$$

where the noise satisfies

$$\langle f(t)f(t')\rangle = 2\eta k_B T\delta(t - t')\,. \tag{4}$$

To ensure this, we pick the bath frequencies ω_α and oscillator strengths f_α to satisfy

$$\frac{\pi}{2\omega}\sum_\alpha f_\alpha\omega_\alpha\delta(\omega_\alpha - \omega) = \lim_{\omega_c\to\infty}\frac{\eta}{1 + (\omega/\omega_c)^2}. \tag{5}$$

We characterize the coupling strength to the bath via the $Q = \Omega_o/2\eta$ of the oscillator, where $\Omega_o = \pi$ is the frequency of small oscillations in the bottom of the well, and concentrate here on the weak-coupling limit $Q \gg 1$.

Since our H_o has a large time-dependent term, neither an imaginary-time path integral formulation of the reduced density matrix [15] nor linear response techniques for treating time-dependent many-body Hamiltonians at finite temperatures [14] are suitable. We therefore studied [24] this problem numerically using a large number of classical oscillators (N=10 000) with fixed oscillator strengths and randomly distributed frequencies chosen to agree with the distribution of Eq. (5), which is justified in the semiclassical limit where the bath is essentially a collection of almost-coherent states [25], each following the classical equations of a very weakly perturbed harmonic oscillator. As the collision rate of the particle with the bath, ω_c in Eq. (5) is chosen to be large compared to the natural frequency of H_o with $\omega_c = 10\Omega_o$.

Finite N means that a given realization of the dynamics will be initial condition-dependent, since all possible realizations of initial conditions for the bath are not represented with a finite number of oscillators. Thus one must finish "tracing out" the initial conditions by averaging over runs, though in practice the need for this depends on the amount of noise in the system as well as N. (With $N = 10\ 000$, about 25 runs were needed before our results stabilized for $Q = 10^3$, as compared to a single run for $Q \geq 10^4$.) Furthermore, because the mean energy per oscillator is not vanishingly small, having N finite sets a minimum temperature—with $\langle H_o \rangle$ a few $k_B T$ above the ground state—so that the bath on average takes energy from the particle. Finally, by requiring that ω_c be no larger than $k_B T/\hbar$, we ensure that even the highest frequency oscillators are relatively classical, but with $\omega_c > \Omega_o$ by an order of magnitude, this also means the temperature is high on the natural scale of the problem.

We use a simple one-step predictor-corrector algorithm [24] to evolve the combined system of quantum particle and semiclassical oscillators forward in time. For the corresponding classical motion we use the phenomenological equations of motion to integrate forward a cloud of initial conditions that represents the phase space probability density $\rho_{cl}(P, X, t)$. This two-dimensional distribution is depicted graphically as a dot plot at snapshots in time and also in reduced form $\rho_{cl}(X, t) = \int \rho_{cl}(P', X, t)\mathrm{d}P'$ as a one-dimensional histogram. The "wave function" $\psi(X, t)$ is then compared to $\rho_{cl}(P, X, t)$ in two ways: by resampling the quantum amplitude $|\psi(X, t)|^2$ to match the bin size of the classical histogram and by projecting $\psi(X, t)$ into phase space using the Husimi transform [26].

In Fig. 2 we compare the one-dimensional distributions $|\psi(X)|^2$ and $\rho_{cl}(X)$ for $Q = \infty$, $Q = 10^4$, and $Q = 10^3$ at a time $t = 13$. The initially equivalent quantum and classical descriptions have begun to differ because of the appearance of the first tendril, which is the folded feature in Fig. 2(a) near $P = -1.0$ superimposed on the spiraling whorl in the region $0.1 < X < 0.4$. The resulting nonclassical nodal structure represents a semiclassical beating phenomenon between the upper branch of the tendril and the remnant separatrix, as discussed earlier.

Note that these nodes, though largely unaffected by the environment for $Q \geq 10^4$ (Fig. 2(b)), seem to have disappeared altogether for $Q = 10^3$ (Fig. 2(c)). This result is interesting, not so much because the presence of an environment suppresses quantum interference (which one expects), but because it happens barely six cycles into the motion, long before dissipation is an appreciable effect ($t \ll Q/\Omega_o$). This is particularly apparent when comparing Figs. 2(a) and 2(c): the nodes disappear without a noticeable shift in the manifold, indicating that the energy of each classical trajectory does not change appreciably. Thus we infer that noise rather than dissipation plays the dominant role in the semiclassical regime for weak damping, where the noise strength varies as $Q^{-1/2}$ while the dephasing by energy loss should vary as Q^{-1} for large Q.

If this semiclassical interpretation of the dephasing is correct, one would expect to see nodal structure associated with the tail of the tendril ($X > 0.4$) where the paths do resolve and the action difference is presumably smooth enough to preserve the coherence. While obscured by a "turning point" in Fig. 2(c), these nodes do in fact appear in the Husimi transform shown in Fig. 3. Note in particular that the primary antinode at $(P, X) \approx (-0.75, 0.45)$ in Fig. 3(a) coincides with where the noisy paths coalesce in Fig. 3(b) rather than at the leading fold of the tendril (*i.e.*, the false caustic) where it occurs for the isolated problem. In addition, we calculated the action difference and found it to be a well-defined quantity in the region where these nodes are observed with the enclosed phase space correctly accounting for the number of nodes [10].

The surprising feature of this structure is that the paths that interfere to produce it would not exist at all without the noise; that is, evolving the cloud with damping but without noise produces no appreciable amplitude here, only the usual (nominal) exponential tail. Moreover, this amplitude does not come from a specific region of the cloud. Rather, cloud particles are kicked (or “filtered”) here “at random” while in the vicinity of the hyperbolic fixed point.

In summary, when we introduce the coupling to the environment, we find that quantum coherence is destroyed for the tendrils first, and that this dephasing is primarily a noise effect. All paths are not affected equivalently, however: some paths retain their coherence, including certain “new” paths that appear because of the noise, while others do not. Noise in “quantum chaos,” like classical chaos [27], thus has a dual role: it assists the mixing by scrambling existing paths but also inhibits the mixing by creating new paths that interfere. These new paths, having crossed the (dynamic) potential barrier associated with a classical turning point, represent noise-assisted tunneling. It is interesting that while these paths arise from the coupling to the environment, they are not dephased as much as those paths that are present without the coupling.

This work was supported by the National Science Foundation under Grant No. DMR–9408634.

REFERENCES

[1] T. Hogg and B. A. Huberman, Phys. Rev. Lett. **48**, 711 (1982); Phys. Rev. A **28**, 22 (1983).

[2] M. C. Gutzwiller, *Chaos in Classical and Quantum Mechanics* (Springer, Berlin, 1990); L. E. Reichl, *The Transition to Chaos* (Springer, New York, 1992).

[3] G. Casati and B. V. Chirikov, Phys. Rev. Lett. **75** 350 (1995); W. H. Zurek and J. P. Paz, Phys. Rev. Lett. **75** 351 (1995).

[4] W. H. Zurek and J. P. Paz, Phys. Rev. Lett. **72**, 2508 (1994).

[5] R. Roncaglia, L. Bonci, B. J. West, and P. Grigolini, Phys. Rev. E **51** 5524 (1995).

[6] R. P. Feynman, Rev. Mod. Phys. **20** 367 (1948).

[7] M. V. Berry, N. L. Balazs, M. Tabor, and A. Voros, Ann. Phys. (N.Y.) **122**, 26 (1979).

[8] L. S. Schulman, J. Phys. A **27**, 1703 (1994).

[9] S. Tomsovic and E. J. Heller, Phys. Rev. Lett. **67**, 664 (1991); Phys. Rev. E **47**, 282 (1993).

[10] B. S. Helmkamp and D. A. Browne, Phys. Rev. E **49**, 1831 (1994).

[11] B. S. Helmkamp and D. A. Browne, Phys. Rev. E **51** 1849 (1995).

[12] J. H. Van Vleck, Proc. Nat. Acad. Sci. USA, **14**, 178 (1928).

[13] M. C. Gutzwiller, J. Math. Phys. **8**, 1979 (1967).

[14] U. Weiss, *Quantum Dissipative Systems* (World Scientific, Singapore, 1993).

[15] A. O. Caldeira and A. J. Leggett, Phys. Lett. **46**, 211 (1981); Ann. Phys. (N.Y.) **149**, 374 (1983).

[16] S. Adachi, M. Toda, and K. Ikeda, Phys. Rev. Lett. **61**, 655 (1988).

[17] E. Ott and T. M. Antonsen, Jr., Phys. Rev. Lett. **53**, 2187 (1984).

[18] R. Scharf and B. Sundaram, Phys. Rev. E **49**, 2509 (1994).

[19] E. J. Heller, Phys. Rev. Lett. **53**, 1515 (1984).

[20] Y. B. Zel'dovich, Zh. Eksp. Teor. Fiz. **51**, 1492 (1966) [Sov. Phys. JETP **24**, 1006 (1967)].

[21] S. Chandrasekhar, Rev. Mod. Phys. **15**, 1 (1943).

[22] R. P. Feynman and F. L. Vernon, Ann. Phys. (N.Y.) **24**, 118 (1963).

[23] W. A. Lin and L. E. Reichl, Phys. Rev. A **31**, 1136 (1985).

[24] B. S. Helmkamp, Ph. D. thesis, Louisiana State University, 1995, Ch. 4.

[25] L. D. Landau and E. M. Lifshitz, *Quantum Mechanics* (Pergamon, Great Britain, 1977), p. 71.

[26] K. Husimi, Proc. Phys. Math. Soc. Jpn. **22**, 264 (1940).

[27] G. Mayer-Kress and H. Haken, J. Stat. Phys. **26**, 149 (1981); K. Matsumoto and I. Tsuda, J. Stat. Phys. **31**, 87 (1983).

FIGURES

FIG. 1. (a) The unperturbed cosine potential with a schematic depiction of the initial wave packet—a coherent state "centered" at $(P_o, X_o) = (-0.397, 0.067)$ with width corresponding to the ground-state wave function. (b) The initial orbit at $E = H_o(P_o, X_o) = -0.331$ (dashed) and the unperturbed separatrix at $E = 0.500$ (solid). The size and "location" of the initial state are given by the three-sigma ellipse at (P_o, X_o). Note the locations of the hyperbolic fixed points (denoted *hfp*).

FIG. 2. A comparison of $|\psi(X,t)|^2$ (solid) and $\rho_{cl}(X,t)$ (dashed) at $t = 13$ for (a) $Q = \infty$, (b) $Q = 10^4$, and (c) $Q = 10^3$. In each case the classical dot plot is shown as well. Note that the oscillations in $|\psi|^2$ corresponding to the folded tendril feature disappear when Q is increased from 10^3 to 10^4 (roughly a three-fold increase in root-mean-square noise).

FIG. 3. The (a) Husimi transform and (b) classical dot plot corresponding to Fig. 2(c) magnified in the region of the tendril. (Contours are on a logarithmic scale.) Note the absence of structure in the Husimi transform at the old location of the false caustic. Also note that the primary antinode occurs where the muddled paths resolve.

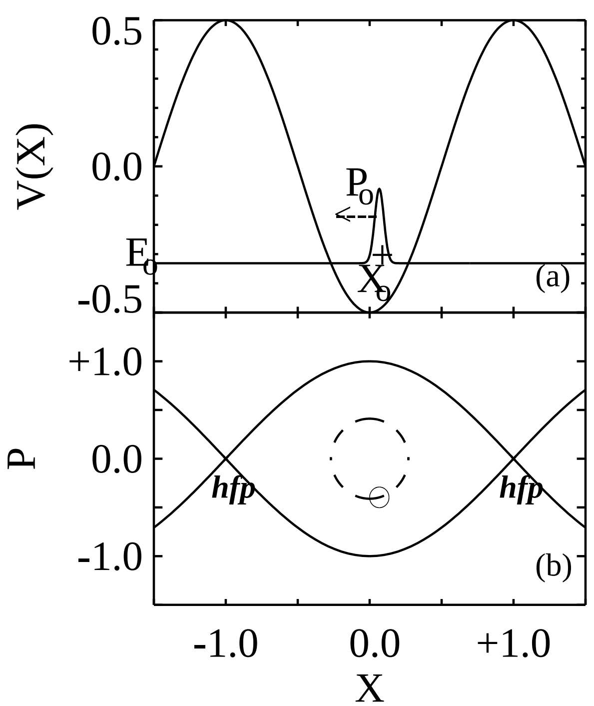

0.5
0.0
-0.5
V(X)
P_o
E_o
X_o
(a)
+1.0
0.0
-1.0
P
hfp
hfp
(b)
-1.0
0.0
+1.0
X

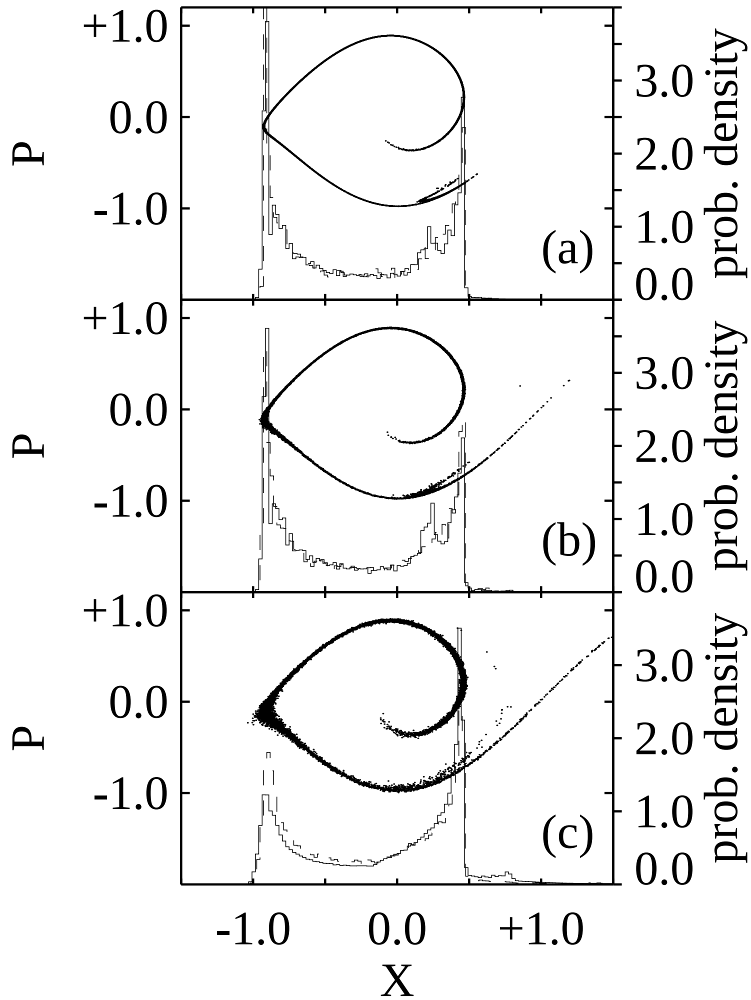

+1.0
0.0
-1.0
P
3.0
2.0
1.0
0.0
prob. density
(a)
(b)
(c)
-1.0
0.0
+1.0
X

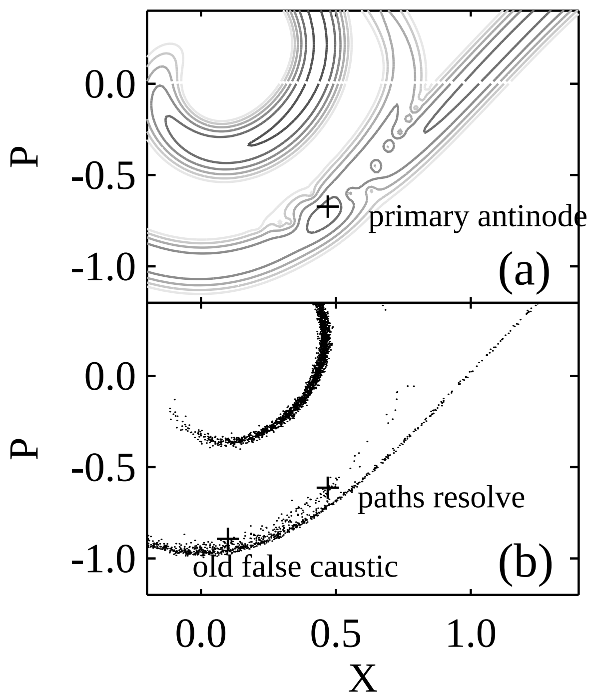

P
0.0
-0.5
-1.0
primary antinode
(a)
P
0.0
-0.5
-1.0
paths resolve
old false caustic
(b)
0.0
0.5
1.0
X